HHS Public Access

Author manuscript

Magn Reson Imaging Clin N Am. Author manuscript; available in PMC 2016 May 01.

Published in final edited form as:

Magn Reson Imaging Clin N Am. 2015 May ; 23(2): 217–229. doi:10.1016/j.mric.2015.01.003.

Hyperpolarized Gas MRI: Technique and Applications

Justus E. Roos,

Department of Radiology, Duke University Medical Center, Box 3808, Durham NC 27710, USA, +1 (919) 684-7325

Holman P. McAdams,

Department of Radiology, Duke University Medical Center, Durham, North Carolina, USA

S. Sivaram Kaushik, and

Department of Radiology, Center for In Vivo Microscopy, Duke University Medical Center & Department of Biomedical Engineering, Duke University, Durham, North Carolina, USA

Bastiaan Driehuys

Department of Radiology, Center for In Vivo Microscopy, Duke University Medical Center, Durham, North Carolina, USA

Justus E. Roos: Justus.roos@duke.edu; Holman P. McAdams: page.mcadams@duke.edu; S. Sivaram Kaushik: sivkaushik@gmail.com; Bastiaan Driehuys: bastiaan.driehuys@dm.duke.edu

Synopsis

Functional imaging today offers a rich world of information that is more sensitive to changes in lung structure and function than traditionally obtained pulmonary function tests. Hyperpolarized helium (^{3}He) and xenon (^{129}Xe) MR imaging of the lungs provided new sensitive contrast mechanisms to probe changes in pulmonary ventilation, microstructure and gas exchange. With the recent scarcity in the supply of ^{3}He the field of hyperpolarized gas imaging shifted to the use of cheaper and naturally available ^{129}Xe. Xenon is well tolerated and recent technical advances have ensured that the ^{129}Xe image quality is on par with that of ^{3}He. The added advantage of ^{129}Xe is its solubility in pulmonary tissue, which allows exploring specific lung function characteristics involved in gas exchange and alveolar oxygenation.

With a plethora of contrast mechanisms, hyperpolarized gases and ^{129}Xe in particular, stands to be an excellent probe of pulmonary structure and function, and provide sensitive and non-invasive biomarkers for a wide variety of pulmonary diseases.

Correspondence to: Justus E. Roos, `Justus.roos@duke.edu`.

Dr. Driehuys is a founder and shareholder of Polarean, Inc. Dr. Roos, Dr. McAdams, and Dr. Kaushik have nothing to disclose.

Keywords

MR imaging; lung imaging; hyperpolarized gas; pulmonary ventilation; pulmonary gas exchange; xenon (^{129}Xe)

1. Introduction

Lung diseases affect the conducting airways, the gas exchange parenchyma or both. As a result, they have a high impact on patients' morbidity, and quality of life. Chronic obstructive pulmonary disease (COPD), for example, is an umbrella term for progressive and irreversible obstructive diseases that affect the airways as well as the parenchyma. After cardiovascular diseases and cancer, COPD is predicted to be the third leading cause of death in the US [1]. Similarly, airway diseases such as asthma have a high prevalence and a large economic impact with $56 billion in associated healthcare costs[2]. Furthermore, interstitial lung diseases (ILD), while less prevalent than COPD or asthma, also have a high morbidity. This is partially attributable to a lack of viable therapeutic options to treat the underlying diseases [3]. However, equally problematic is the lack of sensitive biomarkers that can be used to diagnose these diseases earlier, better monitor progression and show early therapeutic response.

The current gold standard for diagnosis and monitoring treatment of pulmonary diseases is spirometric pulmonary function testing (PFTs). However, by assessing the lung only on a global basis, PFT metrics generally lack the ability to detect functional changes associated with the small airways and gas exchange regions. This insensitivity of PFTs to the functioning of the distal lung (Fig 1) has led these regions to be referred to as the 'silent zone' [4]. Additionally, these metrics largely rely on subject effort, causing significant measurement uncertainty and variability. Hence, current therapy is guided largely by patients' symptoms and survival [5–7]. Given the large burden on our healthcare system and growing prevalence of pulmonary disease, there exists a need for improved diagnostic tools and quantitative metrics to better diagnose and quantify pulmonary disease progression and help accurately measure response to therapy.

To overcome the lungs' many compensatory mechanisms and improve sensitivity to early disease, it is necessary to exploit regional information obtained by imaging. To this end, hyperpolarized (HP) gas magnetic resonance (MR) imaging provides a non-invasive, ionizing-radiation-free method to image pulmonary structure and function [8–13]. While the early days of HP gas MRI saw extensive development and progress using the noble gas ^{3}He, its recent scarcity and concomitant increase in price (~2000$/liter) [14] has caused a transition to the cheaper and naturally available ^{129}Xe (~30$/liter, natural abundance). An added advantage of ^{129}Xe is obtained by virtue of its solubility in pulmonary tissues, which leads to two signal sources, distinct from the xenon in the airspaces. ^{129}Xe can be separately detected in the pulmonary barrier tissues and the red blood cells in the capillary network, compartments in which it exhibits distinct resonant signal frequencies. These three ^{129}Xe resonances can provide quantitative regional information on the fundamental function of the lung – gas-exchange[15].

This article will briefly touch upon the history of HP gas MR imaging, describe the key technical properties, and discuss current and future applications and opportunities for pulmonary imaging.

2. History and Safety

In 1994, the first HP gas MR imaging studies were carried out *ex-vivo* using the noble gas isotope ^{129} Xenon (^{129} Xe)[16]. In 1997, Mugler et al. used ^{129}Xe to conduct the first ground breaking studies in humans [17]. While this represented rapid advancement from mouse to clinical translation, these studies were limited by relatively low ^{129} Xe polarization (1–2%), which resulted in low signal intensities. This caused research interest to transition quickly to the other stable inert gas isotope. ^{3}He, which has a larger gyromagnetic ratio than ^{129}Xe (32.4 MHz/T Vs. 11.77 MHz/T), offered a simpler and more mature polarization technology (~30%), and corresponding larger signal intensities. Additionally, unlike ^{129}Xe which in large enough alveolar concentrations (>70%)[18] is known to exhibit anesthetic properties, ^{3}He does not have any physiological side effects, and was considered to be a better starting point for clinical imaging. Indeed the known anesthetic properties of xenon led to it being regulated as a drug, and further increased the barriers to its use in research. Interestingly, it would later be recognized that the tissue solubility of ^{129}Xe that contribute to its anesthetic properties, actually provided new and exciting opportunities for imaging of the lung beyond what is possible with ^{3}He.

^{3}He MR imaging entered clinical research in 1996[19,20] and soon expanded to multi-center clinical studies [21]. The results of the ventilation studies showed significant correlation to conventional PFTs in patients with COPD, asthma, and cystic fibrosis (CF). Diffusion weighted imaging yielded the apparent diffusion coefficient, which is a sensitive marker of alveolar enlargement, and this marker was significantly increased in subjects with emphysema [8,9,22–24].

The problem with ^{3}He HP MR imaging is twofold. First, the only source of ^{3}He comes from the decay of tritium, which is exclusively derived from the past production of nuclear warheads in the US. The supply from the current stockpile is becoming progressively depleted and access increasingly limited. Secondly, a large portion of the current stockpile has been allocated for homeland security applications to detect emitted neutrons from smuggled plutonium. These reasons have driven up costs significantly to approximately $800–2000 per liter depending on academic versus commercial use [14]. With these higher costs and lower availability, ^{3}He HP MR imaging while having contributed greatly to the creation of this field, is not economically sustainable.

Recent progress in ^{129} Xe polarization technology led Patz et al. to reintroduce ^{129} Xe MR imaging in humans [25]. Xenon has a long history of safe use as a contrast agent in computed tomography (CT) lung imaging studies [26], which was confirmed by Driehuys et al, who rigorously tested the safety and tolerability of inhaling multiple, undiluted 1-liter volumes of hyperpolarized ^{129}Xe [27]. No major adverse effects were reported in total of 44 study subjects including healthy volunteers and COPD patients. Among the reported symptoms were mild dizziness, par-/hypoesthesia and euphoria, which were transient for

approximately 1–2min. No subject showed changes in laboratory tests or ECG. With the advent of more efficient polarizers, resulting in improved ^{129}Xe polarization [28], one can expect better image quality with a lower volume of xenon, and the described symptoms are likely to be diminished further. In fact, a second safety study by Shukla and co-workers showed that inhalation of only 0.5 liter volumes caused subjects to experience few or no symptoms[29].

3. Technique

Traditional MR imaging of the lungs is fraught with a number of difficulties. Conventional MR scanners are primarily tuned to excite hydrogen protons (^{1} H) that are present in abundance in water molecules. However the lungs have only very low ^{1}H density (~20%) compared to other anatomical structures. Combined with a long relaxation time, the signal available for imaging is minimal. Further complicating the image acquisition is the inhomogeneous magnetic environment of the lung, which introduces significant susceptibility artifacts that further challenge conventional MR acquisitions. However, these problems of MR-based lung imaging are not faced by the external gaseous contrast media (^{3}He or ^{129} Xe), which instead image the airways and airspaces within the lungs rather than the surrounding tissues (Fig 2). This greatly reduces the problems of unfavorable longitudinal and transverse relaxation times faced by ^{1}H MRI in the lung. On the other hand, MR imaging of a gas is challenging because it's density is typically about 4 orders of magnitude less than that of protons (^{1}H density of water ~100 Mol/l versus ^{129} Xe gas density ~0.01 Mol/l). This lower density commensurately reduces the available signal intensity and would appear to make gas MRI impossible. To circumvent this limitation, a physical process called hyperpolarization is used to increase the magnetization of these particular gases by about 5 orders of magnitude. Hyperpolarization more than overcomes their low density and makes MR-based imaging of these inhaled gases feasible within a single breath hold.

3.1 Gas Polarization

3.1.1. Physics—The physics around polarizing gases dates back to the atomic physics publications in the 1960's[30,31]. This technology remained of purely intellectual interest until the introduction of high power lasers afforded the ability to polarize large volumes of gases on reasonable time scales. This paved the way for the use of hyperpolarized gases in medical imaging. The schematic shown in Figure 3 describes the sequence of events involved in increasing the nuclear spin polarization of either ^{3}He or ^{129}Xe. This involves two processes – 1) optical pumping, and 2) spin exchange[30,31].

As shown in Fig 3a depicting 6 nuclear spins, under normal conditions, roughly half of the nuclear spins within the gas volume are aligned parallel to the direction of the main magnetic field and half against it. This situation leads to zero signal since the MR signal is determined by the difference in the number of spins aligned in either direction - polarization. Hence, the most ideal scenario that would give us the most signal would have all the nuclear spins pointed along one direction, or 100% polarized. If we were to put this ensemble of spins into a large magnetic field like that of a 1.5T or 3.0T scanner, it would cause slightly more spins to align with rather than against the field. However, this difference while

sufficient for imaging with ubiquitous sources like water, is not nearly sufficient for imaging dilute gases like ^{3}He or ^{129}Xe. An alternative way of viewing our hypothetical system is to note that we need only to add 3 quanta of angular momentum to turn every downward pointed nuclear spin to one that is up and thereby align every nuclear spin in the same direction. Thus, hyperpolarization simply involves adding angular momentum to the system.

To achieve this, circularly polarized laser light is used as a carrier of angular momentum. However, nuclei cannot directly absorb laser light, so we use an intermediary to absorb the light and its angular momentum. Specifically, laser light is tuned to the principal resonance of an alkali metal atom such as rubidium, which causes its single outer-shell valence electron to become aligned. This process is known as optical pumping (Fig 3b) [32,33]. Only alkali metal atoms with electron spins that are down can absorb the light, so simply illuminating the alkali vapor with circularly polarized resonant light will convert the entire sample to the spin up direction. Once a valence electron spin has been flipped up, it remains in this state until collisions cause it to depolarize. But then it simply absorbs another photon and returns to the aligned state.

Subsequently, through collisions between polarized electron spins of the alkali metal rubidium and the ^{129} Xe or ^{3}He nuclei, the alignment from rubidium valence electron is transferred to the noble-gas nucleus. This process is referred as spin exchange (Fig 3c)[30–33]. After the spin-exchange collision, the rubidium electrons become aligned again by absorbing additional laser light and continue to build polarization within the available noble-gas nuclei. Currently available optical pumping and spin exchange techniques deliver polarizations of ~40–80% for ^{3}He and approximately 10 – 40% for ^{129} Xe. Recently, very high peak ^{129}Xe polarization levels have been demonstrated in diluted mixtures [34]

3.1.2. Gas polarization Technique—A simplified schematic for xenon polarization is shown in the Figure 4.

Optical pumping, is carried out using Rubidium (Rb) which is contained within a glass optical cell. This optical cell is housed in an oven, surrounded by two Helmholtz coils that generate a small, but homogeneous 20 G magnetic field. The Rb in the optical cell is heated to ~150° C to produce a Rb vapor pressure equal to about 1ppm of the total gas density in the cell. During this time, 10–100W of circularly polarized laser light tuned to the D1 transition of rubidium illuminates the optical cell. The Rb vapor absorbs a significant fraction (>50%) this incident laser light, which polarizes the valence electron spins on the Rb atoms in the vapor.

Spin exchange is initiated when a mixture of 1% ^{129}Xe, 89% ^{4}He and 10% N_2 is directed to flow through the optical cell and interact with the optically pumped Rb atoms. The buffer gases (helium and nitrogen) serve to pressure broaden the Rb absorption cross section to enable a large fraction of laser light to be productively absorbed. Rb-^{129}Xe spin exchange transfers electron spin polarization to the ^{129}Xe nuclei through a combination of binary collisions and the formation of transient Van der Waals complexes. The gas flow rate through the system is regulated such that ^{129}Xe emerges from the cell highly polarized. To now separate the ^{129}Xe from the ^{4}He and N_2 buffer gases, it is cryogenically accumulated in

a cold finger immersed in liquid nitrogen. As xenon has a higher freezing point than both these gases (~165K), it is selectively frozen out and separated from the helium and nitrogen, which are vented out of the system. Once sufficient xenon has been accumulated, the frozen xenon is thawed, and the gaseous, polarized xenon, is dispensed into a perfluoropolymer bag. The xenon polarization is then measured using a low-field NMR-based system and the delivered to the patient. Commercially available systems can produce liter quantities xenon polarized to 10–15% in 1 hour. New discoveries in polarization physics are certain to enhance both the production rate and ^{129}Xe polarization in the near future.

This dose of xenon is then administered to the subject in the MRI scanner. Prior to inhalation, the subject is coached to inhale to total lung capacity and exhale to functional residual capacity, twice. The contents of the bag are then inhaled through a 6-mm ID Tygon tube which is connected to a mouth piece. Typical scans use between 200-ml and 1000-ml of ^{129}Xe and may be mixed with a buffer gas like helium or nitrogen to create a full inhalation volume.

3.2 MR Scanner Configuration

A conventional MR scanner is typically configured to work primarily on the proton frequency. However, through minor commercially available additions to the MR hardware and software, any scanner can be used to image hyperpolarized gases. As xenon has a gyromagnetic ratio of 11.77 MHz/T which is almost a factor of ~4 lower than that of protons (42.5 MHz/T), at typical field strengths of 1.5 T, it has a much lower resonance frequency of 17.66 MHz. Because most scanners typically use a narrow-banded RF amplifier optimized only for exciting at the proton frequency, non-proton nuclei such as xenon require a separate broad-banded RF amplifier to be installed. Similarly, the receive-side of the scanner is typically also tuned to operate just at the proton frequency and thus must also be broad-banded. Fortunately, such upgrades are available from all major scanner vendors and known as a “multinuclear package”. As with most MR applications, a dedicated transmit-receive coil is also necessary, and must of course be designed to operate at the xenon frequency. It is preferred that such coils are “proton-blocked” to enable an anatomical image to be acquired using the scanners body coil without moving the patient. These RF coils are commercially available (Clinical MR Solutions, WI; Rapid Biomedical, Rimpar Germany) and at our institution we use a quadrature vest coil that delivers optimal SNR (Clinical MR Solutions, WI).

Proton MRI has the advantage of a renewable thermal signal, which affords it the utility of a multitude of MR pulse sequences. However, the non-thermal signal of hyperpolarized gases enforces a number of constraints in the choice of pulse sequences [35]. *Firstly*, once inhaled, the hyperpolarized signal has a finite lifetime in the lung (T_1) which is typically around 20 s. Note that T_1 for hyperpolarized gases refers to timescale with which the polarized state decays down to negligibly small thermal equilibrium values, rather than the conventional beneficial recovery of longitudinal magnetization. The T_1 of xenon in lung is primarily affected by dipolar interactions with paramagnetic, molecular oxygen. Fortunately, T1 effects are rendered somewhat negligible by acquiring images as rapidly as the scanner will allow. A second significant consideration is that the RF pulses used to excite the xenon

signal also deplete its magnetization by the cosine of the flip-angle applied. Hence, a traditional spin echo pulse sequence using 90° and 180° RF pulses cannot generally be used for HP gas imaging. *Secondly*, being a gaseous contrast agent, xenon also has high diffusivity that can depend on the local gas composition (0.14 cm^2/s at infinite dilution) [23,36]. This means that the gradients applied just to acquire the image can actually induce diffusion-based attenuation of the signal if not properly considered. *Lastly*, clinical imaging using hyperpolarized gases require that the acquisition be completed in a short breath-hold (~15 s). These factors confine hyperpolarized gas imaging to fast pulse sequences with low flip angles that can adequately sample all of k-space while minimizing image blurring. This means that most HP gas imaging is done using fast gradient echo based sequences.

4. Clinical Applications

4.1. Ventilation Imaging

The technical robustness and performance of HP ^{3}He gas MR imaging of the lungs was confirmed in multiple clinical studies since its introduction in 1997 [19,20]. HP ^{3}He MRI was predominately applied to produce spin density images of the gas distribution in order to quantify regions that lack any ventilation – ventilation defects. These defects may be caused by obstruction of airways as seen in diseases like asthma, or it may be due to alveolar tissue destruction as seen in emphysema. Given the wide dynamic range of signal intensities in the ventilation images, these intensities can be grouped into 4 clusters to analyze the signal distribution. Clusters of low or absent MR signal within the lungs corresponded well to ventilation defects and allowed to detect and quantify functional ventilation impairment like in asthma, COPD or cystic fibrosis (CF) patients (Fig 5). Since data acquisition is completed during a single breath-hold, this renders static ventilation information from early in the wash-in period. Other dynamic ventilation properties, such as gas flow characteristics including delayed gas filling, are not as readily attainable although significant progress has been made recently in this arena [37].

Traditionally, because of the significantly larger polarization available using HP ^{3}He compared to ^{129}Xe, the ^{3}He image quality was superior. More recently, significant advances in the polarization technology and careful tuning of the MR acquisition have yielded ^{129}Xe ventilation images that rival those obtained with ^{3}He. And as for ventilation defects, despite its lower signal to noise ratio, ^{129}Xe with its higher density and lower diffusivity than ^{3}He seems to be more sensitive to ventilation defects [38]. Currently, using a somewhat larger volume of ^{129}Xe (up to 1 liter per scan) counterbalances the decreased SNR of ^{129}Xe compared to ^{3}He (normally 0.1–0.3 liters per scan) (Fig 6).

4.2 Diffusion-weighted Imaging

Diffusion-weighted MRI has been extensively validated, and widely used with hyperpolarized gases to calculate the apparent diffusion coefficient (ADC) of the gas [8,9,22–24]. The ADC image is obtained by acquiring gas images with and without applying diffusion sensitizing gradients. The value of this contrast derives from the fact that the diffusion of the gases is highly constrained by the architecture of the normal lung.

However, in diseases such as emphysema, where airspaces become significantly enlarged, the gases are free to diffuse (Fig 7). Thus, diffusion weighting can differentiate normal from enlarged airspaces by the degree of signal attenuation observed. The signal intensities in the weighted and non-weighted ventilation images are then used to calculate the ADC on a voxel-by-voxel basis. Thus, ADC maps exhibit low values in healthy lung, whereas in emphysematous lungs elevated ADC values are often observed. In fact, in addition to revealing emphysematous changes, ^{3}He or ^{129}Xe ADC values have been shown to be sensitive to early microstructural changes in asymptomatic smokers [8] and in second hand smokers [39]. Even within healthy individuals, ADC MRI has been shown to be sensitive to age–related changes in alveolar size [40]. Clinical comparisons to CT densitometry [41] showed that ADC strongly correlates with DL_{CO} and that ADC measurements may reveal subclinical emphysematous changes before seen on High Resolution CT (HRCT) [8]. While the majority of ADC imaging to date has involved ^{3}He MRI, it has recently been shown that ADC imaging is also feasible with ^{129}Xe. Fig 8 shows examples of ^{129}Xe ADC images acquired in patients with COPD. It illustrates the highly elevated ADC value seen in emphysematous bullae, but also a more subtle distribution in patients where disease is less severe [23].

5. Future applications

5.1. ^{129}Xe Dissolving imaging

Compared to helium, xenon has a lower gyromagnetic ratio, and images have moderately lower SNR. But, the useful and unique property of ^{129} Xe that sets it apart from ^{3}He, comes by virtue of its moderate solubility in pulmonary tissues [18,42] (Fig 9). As a result, xenon diffuses into the alveolar capillary membrane, and when it does, it experiences a distinct frequency shift from the gas-phase of about 3.5 kHz (on a 1.5T scanner) or 198 ppm in relative terms. Xenon diffuses further into the capillary blood stream, where it transiently binds with the hemoglobin in the red blood cells (RBCs), and when it does, it experiences a larger chemical shift of 217 ppm. These two resonances of xenon are known as the ‘dissolved-phase’, and as xenon follows the same gas transfer pathway as oxygen, these resonances to first order, give us information about gas-exchange in the lung. Hence, while the gas-phase resonance of xenon can be used to provide information relating to ventilatory distribution and microstructure (ADC), the dissolved-phase resonances can be used to probe diffusive gas-exchange.

Imaging this dissolved-phase comes with its own set of challenges. *Firstly*, the magnetization or signal intensity in the dissolved-phase is only ~2% of that in the alveolar spaces, or the gas-phase. *Secondly*, in addition to the lower signal intensity, the T_2* of the dissolved-phase is extremely rapid, at ~2 ms [43]. *Lastly*, as the dissolved-phase resonances are ~200 ppm from the gas-phase, which on a 1.5T scanner is about 3.8 kHz, the RF excitation pulses must be made sufficiently frequency-selective so as to not excite the larger gas-phase magnetization pool.

Because of these limitations, the early efforts in imaging the dissolved-phase employed indirect methods such as Xenon polarization Transfer Contrast (XTC) [44]. As the xenon resonances are in dynamic exchange with one another, RF pulses applied to the dissolved-

phase caused slight attenuation of the gas-phase signal. This concept was used to indirectly map out the dissolved-phase distribution. However, with the onset of increased polarization and rapid pulse sequences, this method soon gave way to approaches that imaged the dissolved ^{129}Xe directly. By using frequency-selective RF pulses and a 3D radial pulse sequence, the first dissolved phase images in humans were acquired in 2010 [45]. These images were of a lower resolution due to the small signal intensity of dissolved phase ^{129}Xe but already showed intriguing aspects of lung function. Soon after the introduction of this direct dissolved-phase imaging approach, Mugler et al., showed the merit of acquiring the 'source' gas-phase distribution in the same breath [46]. This ability allowed for the quantification of the dissolved-phase distribution. This was soon extended to using a radial acquisition strategy, which afforded the ability to quantify the impact of posture on the gas-transfer distribution [15]

However, because the pathway xenon follows to reach the RBCs is identical to that of oxygen, it is the ability to separately detect ^{129}Xe transfer to RBCs that is of fundamental importance. The value of doing so, even on a whole-lung basis was recently demonstrated. Spectra of ^{129}Xe in the dissolved phase were acquired in subjects with idiopathic pulmonary fibrosis and exhibited greatly reduced ^{129}Xe transfer to the RBCs compared to that observed in healthy volunteers [15]. This work thus showed that separating the dissolved ^{129}Xe resonances was critical to enable probing diffusion limitation caused by interstitial thickening in the lung. ^{129}Xe measurements correlated strongly with DLCO but also showed that the frequency of the ^{129}Xe RBC resonance may be a sensitive probe of blood oxygenation at the level of the capillary bed. While this work provided a global marker for gas-exchange impairment, it also highlighted the need to separately detect xenon uptake in the barrier tissues and RBCs by imaging.

Separate imaging of ^{129}Xe in barrier and RBCs is a problem that shares similarities to separating fat and water in ^{1}H MRI. Because the two resonances are similarly spaced, one can borrow from the vast library of fat-water separation algorithms. One such approach was employed by Qing et al., who used the Hierarchical IDEAL algorithm to image all three resonances of xenon in a single breath [47]. Alternatively, the 1-point Dixon strategy has also shown promise, and may be more robust against the short T_2* of the dissolved-phase ^{129}Xe signal. This technique was also recently shown to allow imaging all three resonances of xenon in a single breath [48]. One such example of images of xenon in all three compartments is shown in figure 10. Note that in the patient with IPF, numerous focal defects are visible in the Xe-RBC transfer images. These defects correspond well to fibrotic changes seen on CT.

6. Conclusions

While the field of pulmonary medicine has relied for over 100 years on the pulmonary function tests, increasing evidence is mounting that this is not sufficient. Instead, functional imaging now offers a rich world of information that is more sensitive to changes in lung structure and function than PFTs. While MRI may not historically have been the first choice to image the lungs, hyperpolarized ^{3}He and ^{129}Xe have begun to change this view. These gases have provided new sensitive contrast mechanisms to probe changes in pulmonary ventilation, microstructure and gas exchange. Given the recent scarcity in the supply of

helium and the associated increase in price, the field has adopted the cheaper and naturally available xenon. Xenon has been shown to be well tolerated in healthy volunteers and subjects with disease, and recent technical advances have ensured that the xenon image quality in on par with that of helium. The added advantage of xenon is that it exhibits two distinct new resonances that permit tracking its diffusion into the barrier tissues and the RBCs. Careful investigation of the amplitude, width and the frequency of these resonances carries additional important information about alveolar oxygenation that is only now beginning to be understood. Perhaps, most importantly, the past several years have now demonstrated that the day has arrived where ^{129}Xe can be imaged 3-dimensionally in all three compartments of the lung (airspace, barrier, RBC) to provide a fundamental view of pulmonary gas-exchange without requiring ionizing radiation. With a plethora of contrast mechanisms, hyperpolarized gases and ^{129}Xe in particular, stands to be an excellent probe of pulmonary structure and function, and provide sensitive and non-invasive biomarkers for a wide variety of pulmonary diseases. Interestingly, combined with recent advancements in structural imaging of the lung using ^{1}H MRI [49], and 3D perfusion measurements, the day may finally be dawning that MR becomes the modality of choice for evaluating cardiopulmonary function comprehensively and non-invasively.

References

1. Hoyert DL, Xu J. Deaths: preliminary data for 2011. National vital statistics reports. 2012
2. Barnett SBL, Nurmagambetov TA. Costs of asthma in the United States: 2002–2007. Journal of Allergy and Clinical Immunology. Feb; 2011 127(1):145–152. [PubMed: 21211649]
3. Nalysnyk L, Cid-Ruzafa J, Rotella P, Esser D. Incidence and prevalence of idiopathic pulmonary fibrosis: review of the literature. European Respiratory Review. Dec 01; 2012 21(126):355–361. [PubMed: 23204124]
4. Hogg JC, Chu F, Utokaparch S, et al. The nature of small-airway obstruction in chronic obstructive pulmonary disease. The New England journal of medicine. Jul 24; 2004 350(26):2645–2653. [PubMed: 15215480]
5. Ashutosh K, Haldipur C, Boucher ML. Clinical and Personality Profiles and Survival in Patients With COPD. Chest. Feb 01; 1997 111(1):95–98. [PubMed: 8995999]
6. Mahler DA, Mackowiak JI. Evaluation of the Short-Form 36-Item Questionnaire to Measure Health-Related Quality of Life in Patients With COPD. Chest. Jul 01; 1995 107(6):1585–1589. [PubMed: 7781351]
7. Nishimura K, Izumi T, Tsukino M, Oga T. Dyspnea Is a Better Predictor of 5-Year Survival Than Airway Obstruction in Patients With COPD. Chest. Jun 01; 2002 121(5):1434–1440. [PubMed: 12006425]
8. Fain SB, Panth SR, Evans MD, et al. Early Emphysematous Changes in Asymptomatic Smokers: Detection with 3He MR Imaging 1. Radiology. Jul; 2006 239(3):875–883. [PubMed: 16714465]
9. Kirby M, Mathew L, Wheatley A, Santyr GE, McCormack DG, Parraga G. Chronic Obstructive Pulmonary Disease: Longitudinal Hyperpolarized 3He MR Imaging 1. Radiology. Jul; 2010 256(1): 280–289. [PubMed: 20574101]
10. McAdams HP, Palmer SM, Donnelly LF, Charles HC, Tapson VF, MacFall JR. Hyperpolarized 3He-enhanced MR imaging of lung transplant recipients: preliminary results. AJR American journal of roentgenology. Oct; 1999 173(4):955–959. [PubMed: 10511156]
11. McMahon CJ, Dodd JD, Hill C, et al. Hyperpolarized 3helium magnetic resonance ventilation imaging of the lung in cystic fibrosis: comparison with high resolution CT and spirometry. European Radiology. Nov 01; 2006 16(11):2483–2490. [PubMed: 16871384]

12. Mentore K, Froh DK, de Lange EE, Brookeman JR, Paget-Brown AO, Altes TA. Hyperpolarized HHe 3 MRI of the Lung in Cystic Fibrosis. Academic Radiology. Nov; 2005 12(11):1423–1429. [PubMed: 16253854]
13. Salerno M, de Lange EE, Altes TA, Truwit JD, Brookeman JR, Mugler JP II. Emphysema: Hyperpolarized Helium 3 Diffusion MR Imaging of the Lungs Compared with Spirometric Indexes—Initial Experience1. Radiology. Feb; 2002 222(1):252–260. [PubMed: 11756734]
14. Kramer D. For some, helium-3 supply picture is brightening. Physics Today. 2011
15. Kaushik SS, Freeman MS, Yoon SW, et al. Measuring diffusion limitation with a perfusion-limited gas—Hyperpolarized 129Xe gas-transfer spectroscopy in patients with idiopathic pulmonary fibrosis. Journal of Applied Physiology. Sep 15; 2014 117(6):577–585. [PubMed: 25038105]
16. Albert MS, Cates GD, Driehuys B, et al. Biological magnetic resonance imaging using laser-polarized 129Xe. Jul 21; 1994 370(6486):199–201.10.1038/370199a0
17. Mugler JP, Driehuys B, Brookeman JR. MR imaging and spectroscopy using hyperpolarized 129Xe gas: preliminary human results. Magnetic resonance …. 1997
18. Kennedy RR, Stokes JW, Downing P. Anaesthesia and the 'inert' gases with special reference to xenon. Anaesthesia and intensive care. Mar; 1992 20(1):66–70. [PubMed: 1319119]
19. Ebert M, Grossmann T, Heil W, Otten EW, Surkau R. Nuclear magnetic resonance imaging with hyperpolarised helium-3. The Lancet. 1996
20. MacFall JR, Charles HC, Black RD, et al. Human lung air spaces: potential for MR imaging with hyperpolarized He-3. Radiology. Aug; 1996 200(2):553–558. [PubMed: 8685356]
21. van Beek EJR, Dahmen AM, Stavngaard T, et al. Hyperpolarised 3He MRI versus HRCT in COPD and normal volunteers: PHIL trial. The European respiratory journal: official journal of the European Society for Clinical Respiratory Physiology. Dec; 2009 34(6):1311–1321.
22. Chen XJ, Moller HE, Chawla MS, et al. Spatially resolved measurements of hyperpolarized gas properties in the lung in vivo. Part I: diffusion coefficient. Magnetic resonance in medicine: official journal of the Society of Magnetic Resonance in Medicine/Society of Magnetic Resonance in Medicine. Oct; 1999 42(4):721–728.
23. Kaushik SS, Cleveland ZI, Cofer GP, et al. Diffusion-weighted hyperpolarized 129Xe MRI in healthy volunteers and subjects with chronic obstructive pulmonary disease. Magnetic resonance in medicine: official journal of the Society of Magnetic Resonance in Medicine/Society of Magnetic Resonance in Medicine. May; 2011 65(4):1154–1165.
24. Swift AJ, Wild JM, Fichele S, et al. Emphysematous changes and normal variation in smokers and COPD patients using diffusion 3He MRI. European Journal of Radiology. Jul; 2005 54(3):352–358. [PubMed: 15899335]
25. Patz S, Hersman FW, Muradian I, et al. Hyperpolarized (129)Xe MRI: a viable functional lung imaging modality? European Journal of Radiology. Dec; 2007 64(3):335–344. [PubMed: 17890035]
26. Latchaw RE, Yonas H, Pentheny SL, Gur D. Adverse reactions to xenon-enhanced CT cerebral blood flow determination. Radiology. May; 1987 163(1):251–254. [PubMed: 3823444]
27. Driehuys B, Martinez-Jimenez S, Cleveland ZI, et al. Chronic Obstructive Pulmonary Disease: Safety and Tolerability of Hyperpolarized 129Xe MR Imaging in Healthy Volunteers and Patients. Radiology. Feb; 2012 262(1):279–289. [PubMed: 22056683]
28. Ruset IC, Ketel S, Hersman FW. Optical Pumping System Design for Large Production of Hyperpolarized Xe 129. Physical review letters. 2006
29. Shukla Y, Wheatley A, Kirby M, et al. Hyperpolarized 129Xe magnetic resonance imaging: tolerability in healthy volunteers and subjects with pulmonary disease. Academic Radiology. Aug; 2012 19(8):941–951. [PubMed: 22591724]
30. Bouchiat MA, Carver TR, Varnum CM. Nuclear polarization in He 3 gas induced by optical pumping and dipolar exchange. Physical Review Letters. 1960
31. Kastler A. The optical production and the optical detection of an inequality of population of the levels of spatial quantification of atoms. Application to the experiments …. J Phys Radium. 1950
32. Goodson BM. Nuclear magnetic resonance of laser-polarized noble gases in molecules, materials, and organisms. Journal of magnetic resonance (San Diego, Calif: 1997). May; 2002 155(2):157–216.

33. Walker TG, Happer W. Spin-exchange optical pumping of noble-gas nuclei. Reviews of Modern Physics. May; 1997 69(2):629–642.
34. Nikolaou P, Coffey AM, Walkup LL, et al. Near-unity nuclear polarization with an open-source 129Xe hyperpolarizer for NMR and MRI. Proceedings of the National Academy of Sciences of the United States of America. Aug 27; 2013 110(35):14150–14155. [PubMed: 23946420]
35. Zhao L, Albert MS. Biomedical imaging using hyperpolarized noble gas MRI: pulse sequence considerations. Nuclear instruments & methods in physics research. Section A, Accelerators, spectrometers, detectors and associated equipment. 1998; 402:454–460.
36. Driehuys B, Walker J, Pollaro J, et al. 3He MRI in mouse models of asthma. Magnetic resonance in medicine: official journal of the Society of Magnetic Resonance in Medicine/Society of Magnetic Resonance in Medicine. Nov; 2007 58(5):893–900.
37. Marshall H, Deppe MH, Parra-Robles J, et al. Direct visualisation of collateral ventilation in COPD with hyperpolarised gas MRI. Thorax. Jul; 2012 67(7):613–617. [PubMed: 22286930]
38. Svenningsen S, Kirby M, Starr D, et al. Hyperpolarized (3) He and (129) Xe MRI: differences in asthma before bronchodilation. Journal of Magnetic Resonance Imaging. Dec; 2013 38(6):1521–1530. [PubMed: 23589465]
39. Wang C, Mugler JP, de Lange EE, Patrie JT, Mata JF, Altes TA. Lung injury induced by secondhand smoke exposure detected with hyperpolarized helium-3 diffusion MR. Journal of Magnetic Resonance Imaging. Feb; 2014 39(1):77–84. [PubMed: 24123388]
40. Fain SB, Altes TA, Panth SR, et al. Detection of age-dependent changes in healthy adult lungs with diffusion-weighted 3He MRI. Academic Radiology. Nov; 2005 12(11):1385–1393. [PubMed: 16253850]
41. Diaz S, Casselbrant I, Piitulainen E, et al. Validity of apparent diffusion coefficient hyperpolarized 3He-MRI using MSCT and pulmonary function tests as references. European Journal of Radiology. Aug; 2009 71(2):257–263. [PubMed: 18514455]
42. Weathersby PK, Homer LD. Solubility of inert gases in biological fluids and tissues: a review. Undersea biomedical research. Dec; 1980 7(4):277–296. [PubMed: 6262972]
43. Mugler, JP.; Altes, TA.; Ruset, IC., et al. Image-based measurement of T2* for dissolved-phase Xe129 in the human lung. International Society for Magnetic Resonance in Medecine; 2012.
44. Ruppert K, Brookeman JR, Hagspiel KD, Mugler JP. Probing lung physiology with xenon polarization transfer contrast (XTC). Magnetic Resonance in Medicine. Sep 01; 2000 44(3):349–357. [PubMed: 10975884]
45. Cleveland ZI, Cofer GP, Metz G, et al. Hyperpolarized 129Xe MR Imaging of Alveolar Gas Uptake in Humans. PLoS One. Aug 16.2010 5(8):e12192. [PubMed: 20808950]
46. Mugler JP, Altes TA, Ruset IC, et al. Simultaneous magnetic resonance imaging of ventilation distribution and gas uptake in the human lung using hyperpolarized xenon-129. Proceedings of the National Academy of Sciences of the United States of America. Dec 14; 2010 107(50):21707–21712. [PubMed: 21098267]
47. Qing K, Ruppert K, Jiang Y, et al. Regional mapping of gas uptake by blood and tissue in the human lung using hyperpolarized xenon-129 MRI. Journal of Magnetic Resonance Imaging. Mar; 2014 39(2):346–359. [PubMed: 23681559]
48. Kaushik, SS.; Robertson, SH.; Freeman, MS., et al. Imaging Hyperpolarized 129Xe Uptake in Pulmonary Barrier and Red Blood Cells Using a 3D Radial 1-Point Dixon Approach: Results in Healthy Volunteers and Subjects with Pulmonary Fibrosis. International Society for Magnetic Resonance in Medecine; 2014.
49. Johnson KM, Fain SB, Schiebler ML, Nagle S. Optimized 3D ultrashort echo time pulmonary MRI. Magnetic Resonance in Medicine. Nov; 2013 70(5):1241–1250. [PubMed: 23213020]

Key points

- Hyperpolarized helium (^{3}He) and xenon (^{129}Xe) MR imaging of the lungs provided sensitive contrast mechanisms to probe changes in pulmonary ventilation, microstructure and gas exchange.
- Recent scarcity in the supply of ^{3}He shifted the field of hyperpolarized gas imaging to the use of cheaper and naturally available ^{129}Xe.
- Xenon (^{129}Xe) has been shown to be well tolerated in healthy volunteers and patients with various pulmonary diseases.
- Current technology allows ^{129}Xe to be imaged 3-dimensionally in all three compartments of the lung (airspace, barrier, red blood cells) and provides a fundamental new view of pulmonary gas-exchange.

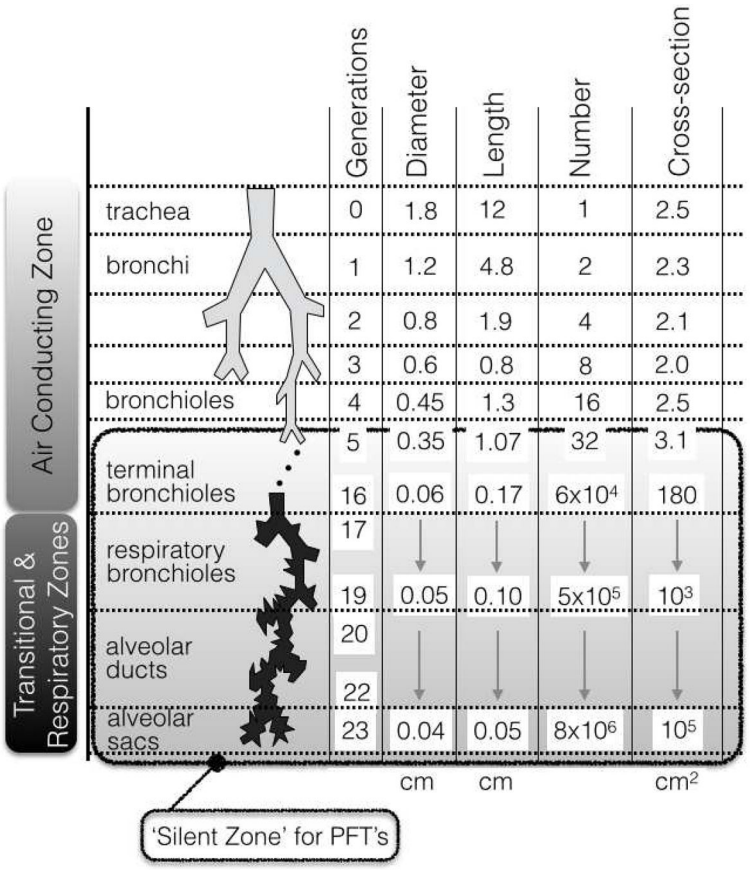

Figure 1.

Anatomical relationship between the purely air conducting zone and the transitional/ respiratory zones. Pulmonary function test (PFTs) lack the ability to detect early changes at the level of the small airways, the so-called ‘silent zone’ for PFTs.

Adapted from Weibel E.R. Morphometry of the Human Lung. Heidelberg Springer, 1963; 111, with permission.

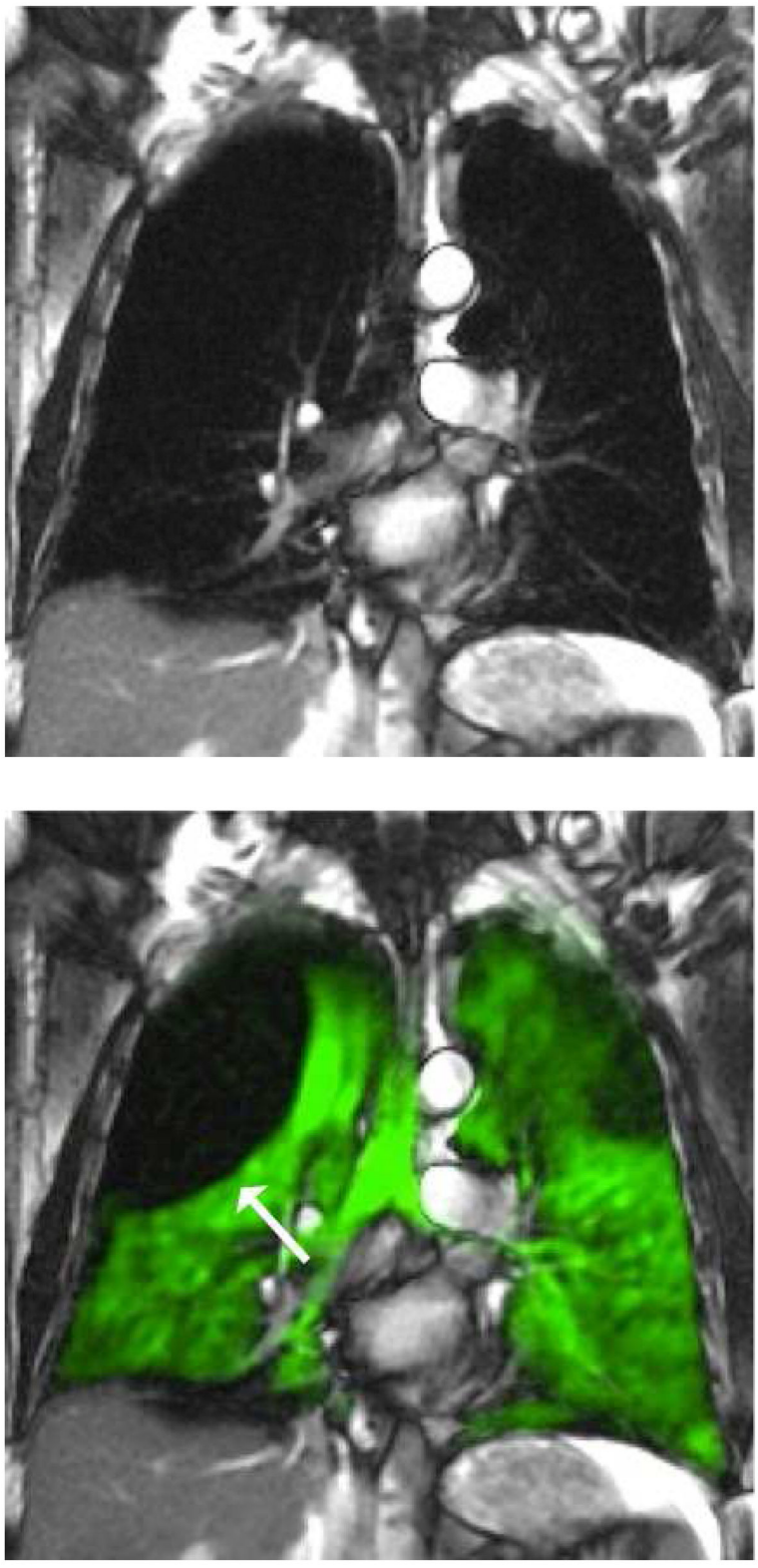

Figure 2.

Coronal mid lung proton MR image without (a) and with (b) hyperpolarized ^{129} Xe Gas contrast (green overlay). It is obvious that proton MR imaging and the lungs are not really close friends: Conventional MR imaging excites and detects hydrogen nuclei (protons) in water. The lungs have a very low proton density and those that are present are difficult to image given their unfavorable relaxation characteristics. However, beyond the challenge of imaging parenchymal structure by MRI, there is an enormous need to image its *function*. This led to the development of contrast techniques using noble gases such as ^{3}He or ^{129} Xe, which nicely demonstrate the lack of ventilation in a large right upper lobe bullae (arrow) in this patient.

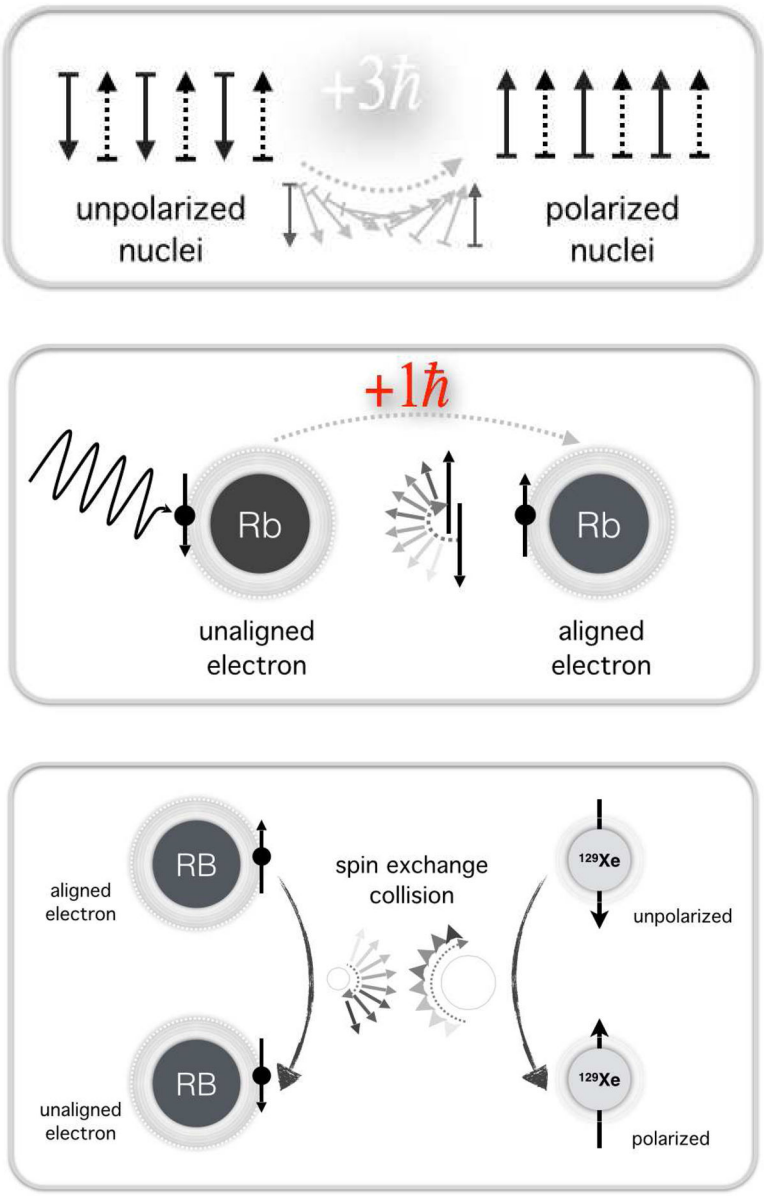

Figure 3.

Schematics explain sequence involved in gas polarization. Under normal conditions, half of the nuclear spins within the gas volume are pointed up, along the magnetic field direction, and half are pointed down. This leads to zero polarization. If we put this sample in a large magnetic field (1.5 – 3.0 Tesla), it is slightly more favorable for spins to be up, but this leads to polarization of only a few parts per million. In hyperpolarization, we seek to have nearly all nuclei spins polarized in one direction. As shown in panel (a), from a physics perspective, all that is needed to transform this unpolarized sample of 3 down and 3 up spins, is to add 3 quanta of angular momentum (a) to flip the down spins to up, and polarize the sample. (b) We cannot directly flip nuclear, but we can flip electron spins in an alkali metal atom rubidium, which by absorbing angular momentum from laser photons, allows its outer-shell valence electron to become spin polarized. This process is known as optical

pumping (Fig 3b). (c) Mother Nature takes care of the rest when ^{129}Xe or ^{3}He nuclei collide with Rb and transfer polarization from its valence electron to the nuclear spin of the noble gas atom. This process is known as spin exchange.

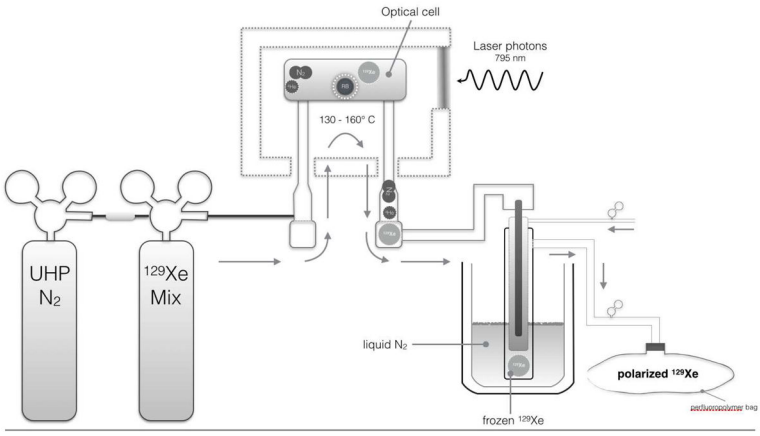

Figure 4.

Schematic of the device used to hyperpolarize ^{129} Xe. The optical pumping and spin-exchange process occurs in the optical cell in a flowing mixture of 1% hyperpolarized ^{129} Xe, 89% ^{4}He and 10% N_2. Once the mixture flows out of the optical cell, ^{129} Xe can be separated from the ^{4}He N_2 buffer gases by exploiting the fact that xenon freezes readily at the 77 K temperature of liquid nitrogen, while the other gases remain gaseous. Once a sufficient quantity of HP ^{129} Xe has been frozen and accumulated, it is thawed and evacuated into a perfluoropolymer bag for delivery to the patient and subsequent imaging. In these bags, the hyperpolarized state has about a 1 hour half life, allowing ample time for delivery.

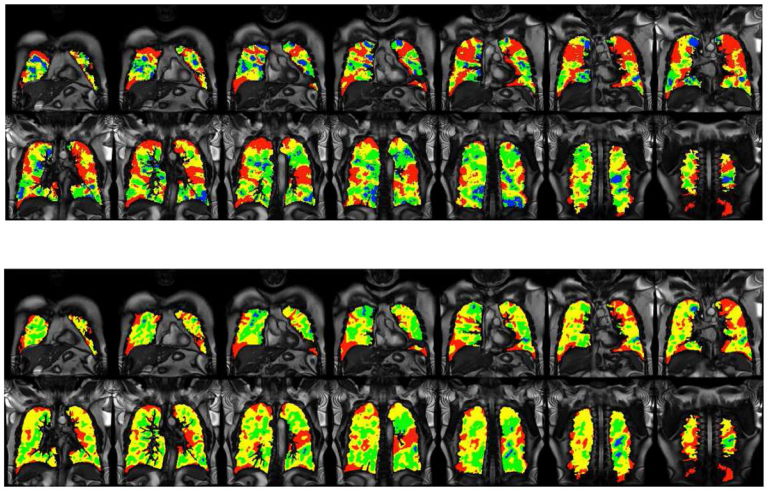

Figure 5.

Quantified ventilation defects using a 4 color ventilation mask with color red representing the most impaired ventilation in a asthma patient Pre (a) and Post (b) bronchodilator therapy. From these images, the ventilation defect percentage (VDP) can be calculated. In this patient with FEV1=31%, the pre-bronchodilator VDP = 30%; post-bronchodilator, the FEV_1 remained at 31%, while VDP reduced significantly to 19%. Based on ATS criteria patient would represent a non-responder to bronchodilatation by PFT criteria, while quantified HP gas ventilation confirms a significant and positive effect to bronchodilator therapy.

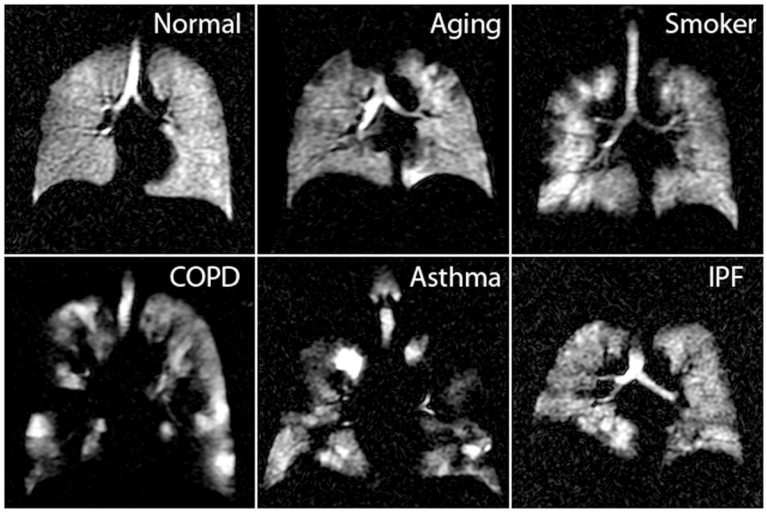

Figure 6.

Hyperpolarized ^{3}He ^{129}Xe images of healthy volunteer, old but otherwise healthy individual, smoker without COPD, COPD, asthma and IPF patients. Hyperpolarized ^{129}Xe images accurately depict different ventilation patterns related to underlying pulmonary disease.

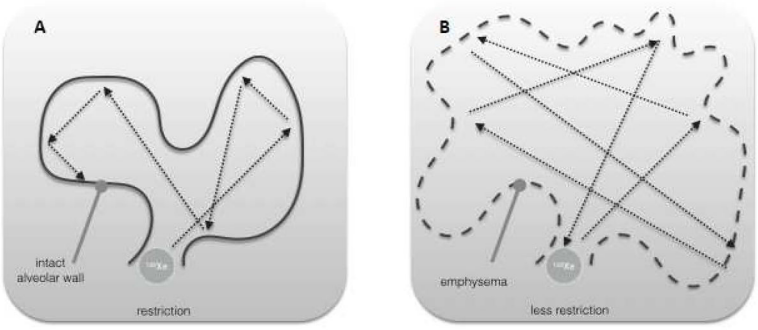

Figure 7.

Diffusion-weighted imaging of hyperpolarized ^{129} Xe can reveal airspace enlargement. The schematics compares diffusion of gas atoms in normal lung airspaces (a) versus enlarged airspaces (b). In normal airspaces the diffusion of ^{129}Xe is constrained by the normal alveolar architecture. However, when alveolar spaces become enlarged such as occurs in emphysema, ^{129}Xe diffusion is no longer constrained, and measured apparent diffusion coefficients (ADC) become higher.

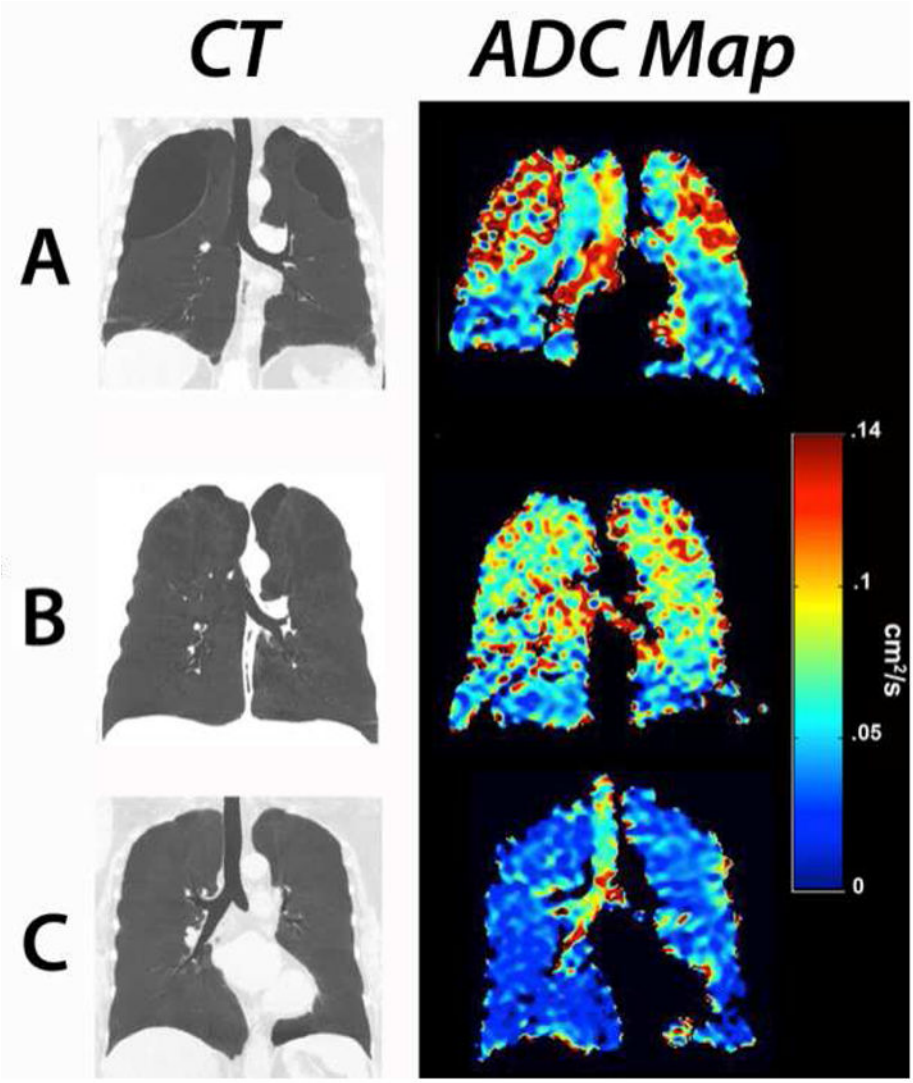

Figure 8.

Apparent diffusion coefficient (ADC) MRI using HP ^{129} Xe gas. The color scale shows escalating enlargement of airspaces from normal lung tissue (blue) to severe bullous emphysematous parenchymal destruction (red). Note parenchymal destruction depicted by CT paralleling the change of ADC values.

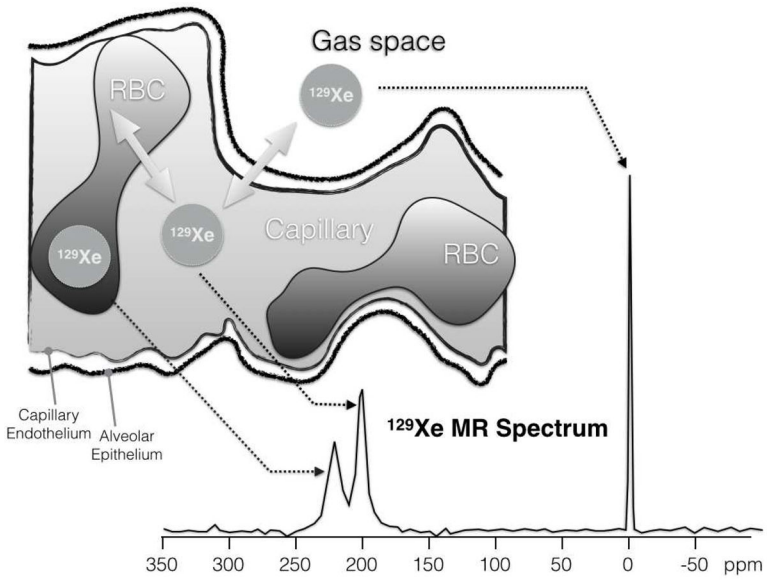

Figure 9.

Hyperpolarized ^{129}Xe can be separately detected in airspaces, interstitial tissues, and red blood cells (RBCs). A small fraction of the inhaled ^{129}Xe dissolves in pulmonary tissues and blood plasma (referred to as the barrier tissues), and changes its MR frequency dramatically compared to ^{129}Xe left in the airspaces. When ^{129}Xe diffuses further into the RBCs it changes its detection frequency again. Because ^{129}Xe follows essentially the same pathway as oxygen, these spectroscopic properties of ^{129}Xe present an enormously powerful means to directly assess pulmonary gas exchange.

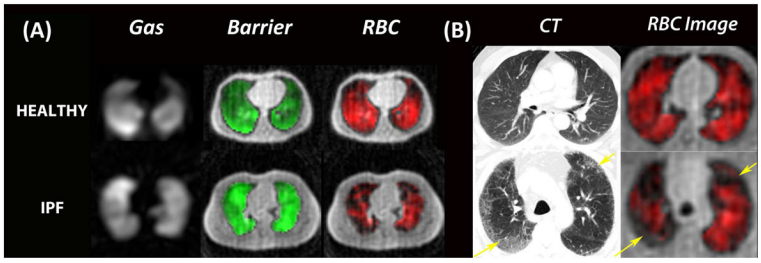

Figure 10.

Dissolved Hyperpolarized ^{129}Xe MR imaging in healthy individual and patient with idiopathic pulmonary fibrosis (IPF).

(a) Recent improvements in 3D radially acquired, breath-hold images of inhaled ^{129}Xe now enable simultaneous depiction of ^{129}Xe in airspaces as well as ^{129}Xe transfered to the barrier and RBC compartments. (b) Note that in the patient with IPF, numerous focal defects are visible in the Xe-RBC transfer images. These defects nicely correspond to fibrotic changes seen on CT (yellow arrows).